View metadata, citation and similar papers at core.ac.uk
brought to you by CORE
provided by PolyU Institutional Repository

APPLIED PHYSICS LETTERS **88**, 182905 (2006)

Comparison of interfacial and electrical characteristics of HfO_2 and HfAlO high-*k* dielectrics on compressively strained $Si_{1-x}Ge_x$

K. K. S. Curreem, P. F. Lee, K. S. Wong, and J. Y. Dai[a)]
Department of Applied Physics, The Hong Kong Polytechnic University, Hung Hom, Kowloon, Hong Kong, People's Republic of China

M. J. Zhou, J. Wang, and Quan Li
Department of Physics, The Chinese University of Hong Kong, Shatin, New Territory, Hong Kong, People's Republic of China

(Received 17 January 2006; accepted 19 March 2006; published online 4 May 2006)

Interfacial reactions and electrical properties of HfO_2 and HfAlO high-*k* gate dielectric films on strained $Si_{1-x}Ge_x$ ($x=17\%$) fabricated by pulsed-laser deposition were investigated. The dielectric films were characterized by x-ray photoelectron spectroscopy, transmission electron microscopy, and electrical measurements. We found that alloying of HfO_2 with alumina can reduce the GeO_x formation at the interfacial layer and thus reduce the Ge diffusion during the film post-thermal annealing process. Such suppression effect significantly improved the electrical properties of the dielectric films. © *2006 American Institute of Physics*. [DOI: 10.1063/1.2201887]

In the semiconductor industry, there is an urgent demand for suitable high-*k* dielectric materials to replace SiO_2 as the gate dielectric in the future advanced complementary metal-oxide-semiconductor (CMOS) technology.[1,2] Recent literatures as well as our preliminary results have shown that HfO_2 is one promising high-*k* gate dielectric substitute for SiO_2 due to its thermodynamic stability and low leakage current.[1–8] However, the carrier mobility degradation due to the high-*k* gate dielectric induced phonon and Coulomb scattering effect limits the application of high-*k* gate dielectrics.[2] It has been noticed recently that the use of a compressively strained $Si_{1-x}Ge_x$ surface channel may serve as a solution to the carrier mobility degradation problem.[2,5,9–11]

The main issue in the $HfO_2-Si_{1-x}Ge_x$ system is the interfacial reaction, in particular, the GeO_x formation and Ge diffusion that result in large amounts of interfacial traps and charge traps in the dielectric.[2,12–14] In addition, the relatively low crystallization temperature (about 500 °C) and high oxygen diffusivity of HfO_2 result in a rough interfacial structure and a large leakage current. A good interface which is thermodynamically stable and has low density of states is therefore essential in reducing the scattering effect on the charge carriers in the channel.[9,15,16] It has been illustrated that adding alumina into HfO_2 on Si (forming HfAlO) increases its crystallization temperature and reduces the oxygen diffusivity.[17] However, to the best of our knowledge, there has not been any report demonstrating that HfAlO can also improve the interfacial reaction and electrical property when applied on the $Si_{1-x}Ge_x$ surface channel MOS field effect transistor. In this letter, we report on synthesis and characterizations of HfAlO thin films, in comparison with HfO_2, on compressively strained $Si_{1-x}Ge_x$. The reactions at the film-$Si_{1-x}Ge_x$ interface and the corresponding electrical properties of the MOS capacitors are investigated.

Si substrates with a layer of 15 nm compressively strained *p*-type $Si_{1-x}Ge_x$ ($x=17\%$) on top were first cleaned with dilute hydrofluoric acid solution to remove the native oxide from the surface. The dielectric films were then grown by pulsed-laser deposition (PLD) on the strained $Si_{1-x}Ge_x$ layer with a base pressure of $\sim 2\times 10^{-4}$ Pa and an oxygen partial pressure of 2 Pa at 550 °C using HfO_2 and Al_2O_3 composite target (Hf:Al=1:1). The postannealing was carried out in a N_2 ambient at 600 °C for 45 min. In order to investigate the interfacial chemical structure, another set of samples with very thin (about 1.5 nm) HfO_2 and HfAlO films were deposited on the same substrate for the x-ray photoelectron spectroscopy (XPS) analysis. Such thickness allows an XPS investigation of the film and the interface simultaneously, and thus information on interfacial reactions can be obtained. The interfacial microstructure was observed by transmission electron microscopy (TEM) using a JEOL 2010 electron microscope. For an electrical property characterization, thicker films with thicknesses of about 5 nm were deposited. The MOS capacitor structures on strained $Si_{1-x}Ge_x$ were fabricated by depositing Pt dot electrodes for both as-grown and annealed samples. Both high-frequency (1 MHz) capacitance-voltage (*C-V*) measurement using an HP4194A impedance analyzer and current-voltage (*J-V*) measurement were carried out.

Figure 1(a) shows XPS spectra of the Hf 4*f* binding energies for the HfO_2 and HfAlO thin films before and after thermal annealing. The peak positions were calibrated using C 1s lines as the reference. For the as-grown samples, the two distinct peaks corresponding to the Hf $4f_{7/2}$ and $4f_{5/2}$ of the Hf–O bond are identical, while they become broaden and difficult to resolve for the annealed samples, especially the HfO_2 film. This peak broadening is due to the formation of Hf silicate or germanate at the interface during the thermal annealing.[9] The convolution of Hf silicate and/or germanate peaks with Hf 4*f* peaks results in the broadening of the Hf–O peaks. In addition, very clear differences in the Hf 4*f* peaks can be observed for the annealed HfO_2 and HfAlO films. We believe that the relatively less broadening effect for the annealed HfAlO film compared to that for the annealed HfO_2 film can be attributed to the fact that the presence of Al in the film reduces oxygen diffusion in the film and thus reduces the formation of Hf silicate and germanate at the interface.

[a)]Author to whom correspondence should be addressed; electronic mail: apdaijy@inet.polyu.edu.hk

0003-6951/2006/88(18)/182905/3/$23.00

© 2006 American Institute of Physics
Downloaded 31 Mar 2011 to 158.132.161.52. Redistribution subject to AIP license or copyright; see http://apl.aip.org/about/rights_and_permissions

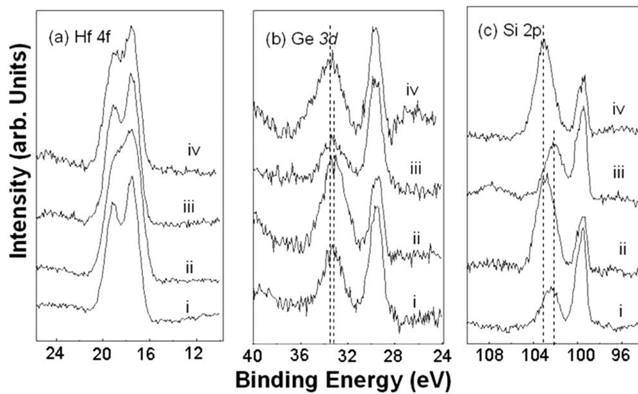

FIG. 1. XPS spectra of Hf 4f (a), Ge 3d (b), and Si 2p (c) binding energies for the films of HfO_2 as-grown (i), HfO_2 after annealed (ii), HfAlO as-grown (iii), and HfAlO after annealed (iv).

Figure 1(b) shows the XPS spectra of Ge 3d binding energies for the HfO_2 and HfAlO thin films before and after thermal annealing. Curve fittings of the Ge 3d core level spectra reveal two peaks corresponding to chemical bindings of Ge in elemental Ge and GeO_x, respectively. The main peak at the binding energy of ~29.3 eV originates from the elemental form of Ge in the $Si_{1-x}Ge_x$ substrate, and the peak at the higher binding energy indicates the presence of GeO_x resulting from the Ge oxidation at the interfacial region. By comparing the peak intensities between the as-grown and annealed HfO_2 samples, one can find the significant increment of the GeO_x peak intensity which indicates a severe oxidation of Ge at the $HfO_2-Si_{1-x}Ge_x$ interface after thermal annealing. On the other hand, for the annealed HfAlO film, there is only a small increment of the GeO_x peak intensity, and the Ge peak is still higher than the GeO_x peak, suggesting that adding alumina into HfO_2 suppresses further oxidation of Ge at the $HfAlO-Si_{1-x}Ge_x$ interface. In addition, a very careful examination of the binding energy of the GeO_x peak of the four samples reveals that there is a slightly higher energy shift (~0.4 eV) for the annealed HfAlO film [Fig. 1(b)(iv)] compared to the other three. The higher binding energy of Ge can be attributed to the more fully oxidized Ge,[9] and thus more energy is needed to break the bond resulting in a higher thermal stability and a lower diffusivity of Ge compared to GeO.[16] This Ge diffusion suppression effect is also revealed by the absence of a hysteresis loop in the following C-V result. It is interesting to note from Fig. 1(c), however, that this suppression effect is not that obvious for the formation of SiO_x at the interface, suggesting that HfAlO may have some selectivity in suppressing the formation of GeO_x and SiO_x at the interfacial layer.

TEM images revealing the interfacial structures and reactions of the thin HfO_2 and HfAlO films on the strained $Si_{1-x}Ge_x$ layer are shown in Fig. 2. It can be seen that after thermal annealing the interfacial layers formed at the $HfO_2-Si_{1-x}Ge_x$ interface for both the thinner and thicker films are relatively thicker and rougher compared to those at the $HfAlO-Si_{1-x}Ge_x$ interface. This illustrates that the presence of alumina in the HfO_2 films helps to improve the interfacial structure during post thermal annealing. It is also worth noting that after annealing at 600 °C, the HfO_2 film is crystallized, while the HfAlO film remains amorphous. The existence of grain boundaries in the crystallized HfO_2 is believed to be responsible for the formation of a rougher interface since the oxygen diffusion along the grain boundaries is faster than that inside the grains.

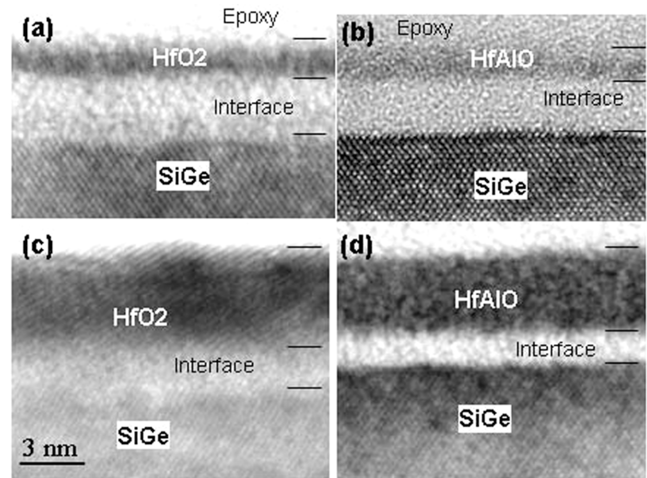

FIG. 2. (Color online) Cross-sectional TEM images showing the interfacial structures for the annealed samples of thin HfO_2 film (a), thin HfAlO film (b), thick HfO_2 film (c), and thick HfAlO film (d) on the compressively strained $Si_{1-x}Ge_x$.

Figure 3 shows the leakage current characteristics of the as-grown and annealed HfO_2 and HfAlO films on $Si_{1-x}Ge_x$. In general, the leakage current densities of HfAlO films are lower than those of HfO_2 films. The large decrease of the leakage current for the annealed films is attributed to the increase of the interfacial layer thickness and the reduction of oxygen deficiencies. The relatively larger leakage current for the annealed HfO_2 film compared to the annealed HfAlO film can be attributed to the crystallization of the HfO_2 oxide layer.[5,18,19]

Figure 4 shows characteristic C-V curves of the as-grown and annealed HfO_2 and HfAlO films on $Si_{1-x}Ge_x$. A significant change can be seen in Fig. 4(a) for the HfO_2 film after annealing. For the as-grown HfO_2 film, there is a large negative flat-band voltage shift (V_{FB}) and a hysteresis loop during forward and reversed bias sweeps. The large negative shift indicates the existence of positive fixed charges in the HfO_2 film. The positive fixed charge in the HfO_2 films has been theoretically explained recently by Robertson[20] and has

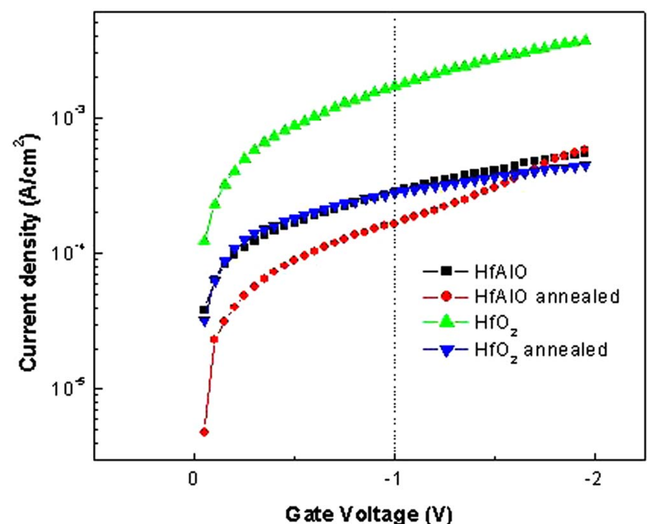

FIG. 3. (Color online) J-V characteristics for the HfO_2 and HfAlO films before and after thermal annealing in a N_2 ambient at 600 °C for 45 min.

Downloaded 31 Mar 2011 to 158.132.161.52. Redistribution subject to AIP license or copyright; see http://apl.aip.org/about/rights_and_permissions

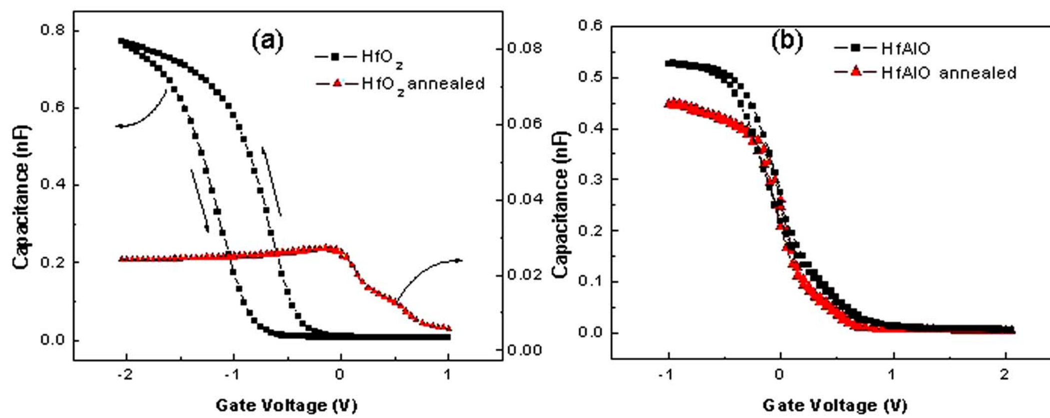

FIG. 4. (Color online) *C-V* characteristics for HfO_2 (a) and HfAlO films (b) before and after thermal annealing in a N_2 ambient at 600 °C for 45 min.

been attributed to oxygen vacancies. Therefore, the right shift of the *C-V* curve after annealing can be explained as a result of the reduction of the number of oxygen vacancies in the HfO_2 film. The large anticlockwise hysteresis loop presented in Fig. 4(a) indicates charge trapping in the oxide, and the diffusion of Ge into the oxide is believed to be responsible for the observed charge storages.[4,19] The oxide trapped charge density (N_{ot}) can be calculated from the *C-V* loop by the following formula:[19]

$$N_{ot} = \frac{C_{acc}\Delta V_{FB}}{qA},$$

where C_{acc} is the accumulation capacitance, ΔV_{FB} is the hysteresis width, q is the electron charge, and A is the electrode area. The density of the trapped charges is calculated to be about 7×10^{12} cm^{-2}. Although the hysteresis loop disappears after thermal annealing, the *C-V* curve shows a large stretch-out, indicating the formation of high densities of interface traps. The significant decrease of the accumulation capacitance for the annealed HfO_2 film is due to the formation of thick Si- and Ge-riched interfacial layers. In Fig. 4(b), however, the *C-V* curve is normal with a very small flat-band voltage shift. The change of the accumulation capacitance of the HfAlO film after annealing is also very small, indicating a very small reduction of the dielectric constant of the film due to the relatively small increment of the $HfAlO-Si_{1-x}Ge_x$ interfacial layer thickness. The effective dielectric constants (including the interfacial layer) of the as-grown and annealed HfO_2 films derived from Fig. 4 are about 16 and 5, respectively, while they are 11 and 9, respectively, for the as-grown and annealed HfAlO films. It is apparent that adding alumina into HfO_2 improves the interfacial property with a sacrificed value of the dielectric constant.

The merit of adding alumina in HfO_2 can be considered in terms of the suppression of the interfacial reactions and Ge diffusion. The XPS and *C-V* results suggest that the presence of alumina in the HfO_2 films reduces the interfacial reaction, which is evidenced by the relatively lower Ge–O peak and smaller interfacial layer thicknesses and roughnesses. Even though TEM results do not show distinct differences in interfacial layer thickness, the fact of having less GeO_x presence in the XPS result and the disappearance of the hysteresis loop in the *C-V* measurement suggest that adding alumina in HfO_2 may reduce the Ge diffusion into the dielectric layer, as alumina serves as an effective diffusion barrier.

In conclusion, the suppression of the GeO_x formation and the Ge diffusion has been achieved by adding alumina into the HfO_2 gate dielectric film on the strained $Si_{1-x}Ge_x$. The corresponding electrical performance has also been improved, as evidenced by the decrease of the leakage current and charge traps in the dielectric layer.

This project is supported by the Hong Kong RGC grant (No. B-Q772).

[1]G. D. Wilk, R. M. Wallace, and J. M. Anthony, J. Appl. Phys. **89**, 5243 (2001).
[2]T. C. Chen, L. S. Lee, W. Z. Lai, and C. W. Liu, Mater. Sci. Semicond. Process. **8**, 209 (2005).
[3]C. K. Maiti, S. K. Samanta, S. Chatterjee, G. K. Dalapati, and L. K. Bera, Solid-State Electron. **48**, 1369 (2004).
[4]S. H. Jeong, Y. Roh, N. E. Lee, and C. W. Yang, Surf. Coat. Technol. **200**, 258 (2005).
[5]J. H. Lee, S. Maikap, D. Y. Kim, R. Mahapatra, S. K. Ray, Y. S. No, and W. K. Choi, Appl. Phys. Lett. **83**, 779 (2003).
[6]J. Kim, S. Kim, H. Jeon, M. H. Cho, K. B. Chung, and C. Bae, Appl. Phys. Lett. **87**, 053108 (2005).
[7]P. F. Lee, J. Y. Dai, K. H. Wong, H. L. W. Chan, and C. L. Choy, Appl. Phys. Lett. **82**, 2419 (2003).
[8]D. Y. Cho, K. S. Park, B. H. Choi, and S. J. Oh, Appl. Phys. Lett. **86**, 041913 (2005).
[9]J. F. Damlencourt, O. Weber, O. Renault, J. M. Hartmann, C. Poggi, F. Ducroquet, and T. Billon, J. Appl. Phys. **96**, 5478 (2004).
[10]M.-H. H. Tae-Hyoung Moon, Appl. Surf. Sci. **240**, 105 (2004).
[11]M. S. Kim, Y. D. Ko, M. S. Yun, J. H. Hong, M. C. Jeong, J. M. Myoung, and I. G. Yun, Mater. Sci. Eng., B **B123**, 20 (2005).
[12]T. J. Park, S. K. Kim, J. H. Kim, J. Park, M. J. Cho, S. W. Lee, S. H. Hong, and C. S. Hwang, Microelectron. Eng. **80**, 222 (2005).
[13]M. Houssa, B. De Jaeger, A. Delabie, S. Van Elshocht, V. V. Afanas'ev, J. L. Autran, A. Stesmans, M. Meuris, and M. M. Heyns, J. Non-Cryst. Solids **351**, 1902 (2005).
[14]Z. H. Shi, D. Onsongo, and S. K. Banerjee, Appl. Surf. Sci. **224**, 248 (2004).
[15]K. I. Seo, P. C. McIntyre, S. Sun, D. I. Lee, P. Pianetta, and K. C. Saraswat, Appl. Phys. Lett. **87**, 042902 (2005).
[16]N. Lu, W. Bai, A. Ramirez, C. Mouli, A. Ritenour, M. L. Lee, D. Antoniadis, and D. L. Kwong, Appl. Phys. Lett. **87**, 051922 (2005).
[17]H. Y. Yu, N. Wu, M. F. Li, C. X. Zhu, B. J. Cho, D. L. Kwong, C. H. Tung, J. S. Pan, J. W. Chai, W. D. Wang, D. Z. Chi, C. H. Ang, J. Z. Zheng, and S. Ramanathan, Appl. Phys. Lett. **81**, 3618 (2002).
[18]V. Mikhelashvili, R. Brener, O. Kreinin, B. Meyler, J. Shneider, and G. Eisenstein, Appl. Phys. Lett. **85**, 5950 (2004).
[19]K. Kukli, M. Ritala, T. Sajavaara, J. Keinonen, and M. Leskelä, Thin Solid Films **416**, 72 (2002).
[20]J. Robertson, Solid-State Electron. **49**, 283 (2005).

Downloaded 31 Mar 2011 to 158.132.161.52. Redistribution subject to AIP license or copyright; see http://apl.aip.org/about/rights_and_permissions